A study of the active thermal control for the high energy detector on the HXMT[*]

ZHANG Yi-Fei(张翼飞)[1)]   LI Yan-Guo(李延国)   WU Bo-Bing(吴伯冰)

ZHANG Yong-Jie(张永杰)   DONG Yong-Wei(董永伟)   SUN Jian-Chao(孙建超)

ZHAO Dong-Hua(赵冬华)   XING Wen(邢闻)   CHAI Jun-Ying(柴军营)

KANG Shi-Xiu(康士秀)   SONG Li-Ming(宋黎明)

Institute of High Energy Physics, Chinese Academy of Sciences, Beijing 100049, China

Abstract: A thermal control system (TCS) based on the resistance heating method is designed for the High Energy Detector (HED) on the Hard X-ray Modulation Telescope (HXMT). The ground-based experiments of the active thermal control for the HED with the TCS are performed in the ambient temperature range from −15 to 20 ℃ by utilizing the pulse width to monitor the interior temperature of a NaI(Tl) crystal. Experimental results show that the NaI(Tl) crystal's interior temperature is from 17.4 to 21.7 ℃ when the temperature of the PMT shell is controlled within (20±3) ℃ with the TCS in the interesting temperature range, and the energy resolution of the HED is maintained at 16.2% @122 keV, only a little worse than that of 16.0% obtained at 20 ℃. The average power consumption of the TCS for the HED with a low-emissivity shell is about 4.3 W, which is consistent with the simulation.

Key words: hard X-ray, HXMT, detector, thermal control

PACS: 95.55.Ka   **DOI:** 10.1088/1674-1137/35/7/008

1 Introduction

The Hard X-ray Modulation Telescope (HXMT) [1], the first Chinese astronomy satellite based on the direct demodulation method, is mainly devoted to performing an energy range 1–250 keV X-ray all-sky imaging survey and researching the deep astrophysical mechanism in black-hole binaries and others. The HED as the primary payload on the HXMT is a NaI(Tl)/CsI(Na) phoswich detector operating between 20 and 250 keV. However, within the expected temperature range from −10 to 45 ℃, the energy resolution of the HED will be degraded significantly caused by the temperature-dependent characteristic of the NaI(Tl) crystal [2, 3]. Pausch et al. [4] have proposed stabilizing the scintillation detector systems by exploiting the temperature dependence of the light pulse decay time, but this method is inefficient due to the unstable correlation of the gamma-ray photoelec-

tric peak and the decay time caused by the change in experimental conditions. Therefore, we adopted the widely used active thermal control methods [5, 6] to directly stabilize the NaI(Tl) crystal's interior temperature to maintain the performance of the HED.

We learnt from early experiments for the HED that the 122 keV gamma-ray photoelectric peak drift is about 10% in the ambient temperature range from −10 to 20 ℃, rather than that of 2% in the range from 20 to 45 ℃. Since the impact of the latter on the energy resolution is negligible compared with the former, only a positive heat compensation for the NaI(Tl) crystal is necessary in the range from −10 to 20 ℃ as the target value of the crystal temperature is about 20 ℃. This situation is suitable for the application of the resistance heating method, one of the active thermal control methods. In this presentation, the ground-based experiments of a thermal control system (TCS) based on this method are carried out

in the ambient temperature range from −15 to 20 ℃ at 1.0 Pa. The NaI(Tl) crystal's interior temperature is traced during the control process, and then the 122 keV gamma-ray photoelectric peak and the energy resolution of the HED are measured. Finally, the average power consumption of the TCS is discussed.

2   Experiment setup

Figure 1 shows a schematic diagram of the ground-based experiment system. The HED, mainly composed of a NaI(Tl)/CsI(Na) phoswich, a Hamamatsu R877 PMT and a preamplifier, is placed in a chamber in which 1.0 Pa pressure is supplied and the temperature ranges from −15 to 20 ℃. A piece of adiabatic syntactic foam board (5 cm thick) is used as the supporter for the HED to avoid heat conduction with the chamber. The TCS consists of a heating belt, a temperature sensor c, a controller and a power supply. The heating belt made up of two polyimide films is wrapped around the PMT shell to make heat compensation for the NaI(Tl) crystal. The power supply is manipulated by the controller, which discriminates between the temperature thresholds T_L, T_H and the PMT shell's temperature T_C measured by the sensor c. The control process is plotted in the lower-left corner of Fig. 1. Temperature sensors labeled a, b, d and e located at the preamplifier, PMT dynodes, PMT cathode and the surface of the entrance window, respectively, are used to depict the temperature distribution of the HED. In order to improve the measurement accuracy, a heat-conducting silicone film of 2 mm in thickness is used as the coupler between each sensor and the corresponding detected area, and the outside sensors c and e are additionally covered over with two pieces of adiabatic syntactic foam to reduce the impact of the surrounding temperature. All five temperature sensors have a precision of 0.2 ℃ in consideration of the electromagnetic interference. An

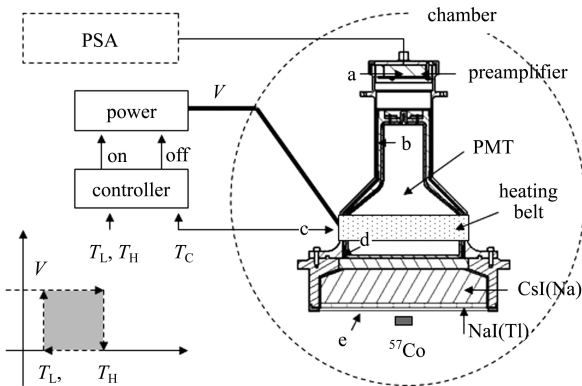un-collimated radioactive isotope ^{57}Co of about 200 Bq is placed at the center of the entrance window of the HED. The output NaI(Tl) signals are analyzed in the PSA [7], event by event, to extract the pulse height and width.

The interior temperature of the NaI(Tl) crystal can directly reflect the control process and help us to evaluate the effect of the TCS. However, the bad thermal conductivity of the NaI(Tl) crystal makes it impossible for those temperature sensors to directly and exactly measure the interior temperature of the air-sealed NaI(Tl) crystal under a thermal non-equilibrium environment. For example, the temperature difference between the inside and the outside of the crystal case reaches up to 4 ℃. Therefore, we develop an effective method of utilizing the pulse width to measure the interior temperature of the NaI(Tl) crystal [8]. This is based on the fact that the pulse width extracted from the given gamma-ray deposited in the NaI(Tl) crystal is almost uniquely dependent on the crystal's operating temperature. In the experiments, the relation between them is calibrated first. At each point of temperature, the test duration of the HED assembly lasts for more than 10 hours to reach complete thermal equilibrium, by the judgement of a steady pulse width spectrum of the NaI(Tl) signals. Since there is no heat source in or beside the NaI(Tl) crystal, its interior temperature is reasonably represented as the average value of T_d and T_e. The relation between the crystal's interior temperature and the pulse width is fitted with a three-order polynomial, as shown in Fig. 2. Based on this relation, the crystal's interior temperature can be measured directly with a maximum error of 0.5 ℃ in thermal equilibrium.
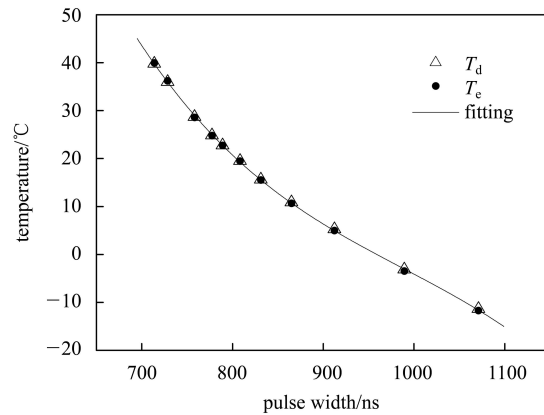

Fig. 2.   Relation between NaI(Tl) pulse width and NaI(Tl) crystal's interior temperature.

In this study, the active thermal control experiments are performed at six stable temperatures of

Fig. 1.   Schematic diagram of the experimental system.

−15 ℃, −8 ℃, −1 ℃, 6 ℃, 12 ℃ and 20 ℃ as the simulated surrounding temperature given by the HXMT changes slowly. At each temperature, three control ranges of (20±1) ℃, (20±2) ℃ and (20±3) ℃ are applied alternately for more than 15 hours.

3 Results and analysis

In the experiments, the 122 keV photoelectric peak and pulse width are calculated statistically every minute. The latter is used to derive the NaI(Tl) crystal's interior temperature according to the fitting curve presented in Fig. 2. The measurement uncertainty of the crystal temperature, due to its

change observed to be less than 0.2 ℃ per minute, is about 0.1 ℃, which can be ignored compared with the measurement error of 0.5 ℃ resulting from this method.

3.1 Control process

In thermal equilibrium without TCS, the power consumption of the preamplifier and the PMT divider in the HED contributes to the distribution of temperature declining from the tail to the entrance window at thermal equilibrium, as shown in Table 1, while the much bigger power consumption of the TCS shifts the temperature vertex adjacent to the heating belt when the HED is controlled with TCS.

Table 1. Temperature distributions of the HED under different conditions at ambient temperature −8 ℃.

conditions	T_a/℃	T_b/℃	T_c/℃	T_d/℃	T_e/℃	T_{crys}/℃
without TCS	5.8	4.2	1.1	1.0	0.8	0.9
controlled with TCS	19.3±0.7	20.9 ±1.0	20.0±3.0	21.0±1.5	19.7±0.4	20.1±1.1

Figure 3 presents the changes in the power voltage, the NaI(Tl) crystal's interior temperature T_{crys} and T_c in the thermal process control. It takes only about 4 hours for the HED assembly to reach a new dynamic equilibrium, in which all of the temperature values and the power voltage act periodically. Additionally, the NaI(Tl) crystal's interior temperature responds a delay $\Delta\tau$ of about 15 minutes to others, which is mainly ascribed to the bad thermal conductivity of the NaI(Tl) crystal. This, to some extent, benefits stabilizing its interior temperature.
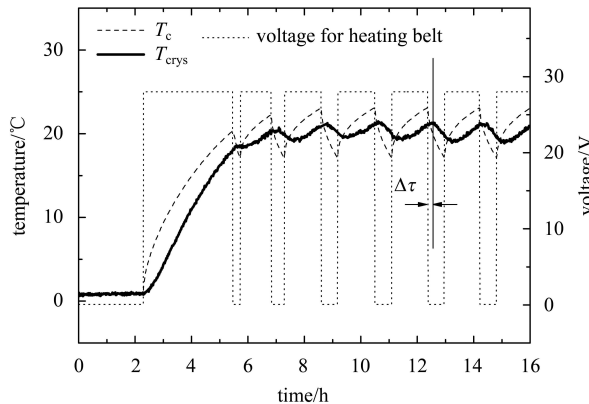

Fig. 3. The control process at ambient temperature −8 ℃.

3.2 NaI(Tl) crystal temperature, photoelectric peak and energy resolution

Table 2 lists the crystal temperature T_{crys}, the relative variation R_{peak} in photoelectric peak and the energy resolution R_{es} (@122 keV) of the HED when the TCS is utilized in the ambient temperature range

from −15 to 20 ℃. The R_{peak} is the ratio of the photoelectric peak variation to the peak measured at 20 ℃, and the energy resolution R_{es} of the HED is derived in accumulation of experimental data acquired in 5 hours duration, when the assembly reaches dynamic equilibrium, at each given ambient temperature.

It is shown that the T_{crys} is controlled to be 17.4 ℃–21.7 ℃ with the temperature control range of (20±3) ℃ on the PMT shell, which has a smaller temperature variation 4.3 ℃ than that of 24.8 ℃ corresponding to the T_{crys}, which is −3.5 ℃–21.3 ℃ measured without TCS. The R_{peak} is 2.4% which is also contributed by the temperature coefficient −0.15%/℃ of the PMT gain apart from the NaI(Tl) crystal, and the R_{es} is maintained to be 16.2%. Both of them are much better than those of 9.5% and 20.5% obtained without TCS.

Table 2. Experimental results obtained in the ambient temperature range from −15 to 20 ℃.

conditions	T_c/℃	T_{crys}/℃	R_{peak}(%)	R_{es}(%)
without TCS	−3.3−21.4	−3.5 − 21.3	9.5	20.5
controlled with TCS	20±1	19.3−20.1	1.5	16.1
	20±2	18.3−20.6	1.8	16.1
	20±3	17.4−21.7	2.4	16.2

Furthermore, as the control range is alternated to be (20±2) ℃ and (20±1) ℃, the variation in T_{crys} shrinks to 2.3 and 0.8 ℃, the R_{peak} to 1.8% and 1.5%, and the R_{es} of the HED becomes 16.1% and 16.1%, close to that of 16.0% measured at 20 ℃. This indicates that proper reduction of the control range helps to improve the performance of the HED, but the improvement is limited.

These results confirm that the TCS based on the resistance heating method is effective in accomplishing the temperature stabilization for the NaI(Tl) crystal and further maintaining the performance of the HED in the ambient temperature range from -15 to 20 ℃.

3.3 Average power consumption of TCS

As shown in Fig. 4, the average power consumption (the product of dutyfactor and maximum power consumption) is negatively correlated with the ambient temperature below 16 ℃. According to the fitting curve in Fig. 4, the average power consumption of the TCS at -10 ℃ is estimated to be about 11.3 W. However, our additional experiment at 10 ℃ shows that about 62% of the average consumption is cut down by wholly insulating the HED with 5 cm thick adiabatic syntactic foam to reduce the thermal radiation from the HED. In this case, the average consumption will be reduced to 4.3 W at -10 ℃, which is consistent with the simulated result 4.5 W for one HED on the HXMT. The implication is that the TCS is applicable to the HXMT.
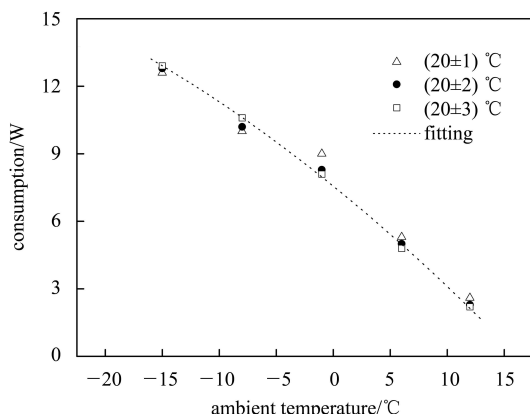

Fig. 4. Average power consumption of the TCS at different ambient temperatures. The dashed line is the fitting curve for the experimental data obtained in the control range of (20±3) ℃.

Moreover, it is evident that the average consumption almost remains invariable as the control range varies. This means that we can reduce the control range to improve the performance of the HED without dissipating more power.

4 Conclusions

The ground-based experiments of the active thermal control for the HED shows that the NaI(Tl) crystal's interior temperature measured with pulse width is controlled by the TCS to be of 17.4 ℃–21.7 ℃ and the resolution (@122 keV) of the HED is maintained to be 16.2% with three control ranges of (20±3) ℃ on the PMT shell in the temperature range from -15 to 20 ℃. By shortening the control range to (20±2) ℃ and (20±1) ℃, the energy resolution is improved by 16.1% and 16.1%, respectively, and it is almost equal to that 16.0% obtained at 20 ℃. These results illustrate the feasibility for the TCS based on the resistance heating method to stabilize the NaI(Tl) crystal's interior temperature so as to maintain the performance of the HED.

Moveover, the current minimum power consumption of the TCS is about 11.3 W at the lowest ambient temperature -10 ℃ given by the HXMT. However, it is experimentally confirmed that it will be reduced to less than 4.3 W when the HED's shell has a lower emissivity. The low power consumption makes the TCS feasible on the HXMT.

Practically, our study is of great benefit to the design of the active thermal control for the HED of the HXMT, and also it can serve as a reference to the thermal controls for other temperature-sensitive inorganic scintillators. Keeping in step with the procedure of the HXMT project, more experiments will be carried out at a target temperature chosen in the range of 18 ℃–25 ℃ with a new low-emissivity shell of the HED instead of utilizing the adiabatic syntactic foam. These will be discussed in the future.

References

1 LI T P. Nucl. Phys. B, 2007, **166**: 131–139
2 Birks J. The Theory and Practice of Scintillation Counting. Oxford: Pergamon Press, 1964. 453–469
3 Knoll G F. Radiation Detection and Measurement. 3rd ed. New York: John Wiley & Sons Inc., 1999. 234–238
4 Pausch G, Stein J, Teofilov N. IEEE Trans. Nucl. Sci., 2005, **52**: 1849–1855
5 HOU Zeng-Qi, HU Jin-Gang. Spacecraft Thermal Control Technology: Princle and Application. Beijing: Science Press, 2007. 273–277 (in Chinese)
6 Gilmore D G. Spacecraft Thermal Control Handbook Volume 1: Fundamental Technologies. 2nd ed. California: Aerospace Press, 2002. 223–246
7 LI Yan-Guo, LI Ti-Bei. Nuclear Electronics & Detection Technology, 2003, **23**: 391–396 (in Chinese)
8 ZHANG Y et al. Nucl. Instrum. Methods A, 2010, **615**: 272–276